Energy loss of a low-energy ion beam in passage through an equilibrium cesium plasma*

D. M. Cox,† H. H. Brown, Jr., I. Klavan,‡ and B. Bederson

New York University, 4 Washington Place, New York, New York 10003

(Received 15 January 1974)

The energy loss of a beam of cesium or lithium ions traversing a near-thermal equilibrium cesium plasma has been measured as a function of plasma density at ion-beam energies of 35–150 eV. The plasma electron-ion temperature ranged from 2100 to 2500 °K, and the charged-particle density ranged from (0.1 to 8.0) $\times 10^{11}$ cm^{-3}. The measured energy loss is found to agree well with theoretical predictions.

I. INTRODUCTION

The simplest and most basic problem in the kinetic theory of plasma physics is the interaction of a single charged particle with a plasma in thermodynamic equilibrium. This "test-particle problem" has received a great deal of theoretical interest.[1] Among the fundamental observables are energy loss or gain and angular deflection of the test particle. In addition, charged-particle beams are potentially very useful analytic and diagnostic tools for plasma-physics research, since they represent a direct means for probing the plasma microfields. Despite the vast theoretical literature, there has been little experimental work performed. The difficulties include the necessarily large magnetic fields confining some plasmas, the usually small magnitude of the energy loss compared to the test-particle energy, sheaths, uncertainties in plasma parameters, inelastic scattering both with plasma constituents and background neutral gas, and additional problems inherent with pulsed plasmas if the plasma is of this type.

We are reporting measurements of the average energy loss of low-density, low-energy (35–150 eV) beams of cesium or lithium ions in passage through a low-density near-thermal equilibrium cesium plasma.[2] The thermal cesium plasma is mechanically confined, has no applied electric or magnetic fields, possesses small thermal and density gradients, and the plasma constituents are almost in full thermodynamic equilibrium with the plasma container. The plasma density and temperature can be varied independently for greater flexibility in experimental measurements.

The quantity of interest, dE/dt, is the rate of energy loss of a test particle owing to its interactions with the plasma particles, and is directly related to the "relaxation time" of a test particle injected into a plasma. The energy-loss rate is of practical interest as the advent of thermonuclear reactors approaches; although the present experimental parameters are in a different range from those necessary for a controlled thermonuclear reactor, a check of the theory in any range will shed light on its general predictions.

II. REVIEW OF PREVIOUS EXPERIMENTAL WORK

Four previous experiments[3–6] are to be compared with the present work. In three experiments, protons (or deuterons) were used for test-particle beams. In the fourth, electrons were used. Reported energy losses ranged from 0.3 to 8 times the value predicted by theory. In all cases the test-particle speed was on the order of, or greater than, the thermal speed of the electrons in the plasma, and very much greater than the ion thermal speeds. In 1965, Smith and Johnson[3] passed 1–3-keV electrons through a helium plasma produced in an electromagnetic shock tube, more commonly called a T tube. The plasma density varied from 5×10^{15} to 1×10^{16} cm^{-3}, with the electron kinetic temperature on the order of 4×10^{4} °K. Experimental results indicated an energy loss $\approx$8 times higher than predicted by their theoretical model.

Ormrod[4] (1967) investigated the energy loss of 30–70-keV protons and 20–70-keV deuterons in an argon hollow-cathode discharge. The plasma was confined by an axial magnetic field of $\approx 10^{3}$ g; the beam path was parallel to the field lines. As measured with a Langmuir probe, the electron density varied from 2 to 11×10^{13} cm^{-3}, and the electron temperature averaged $\approx 6\times10^{4}$ °K. Ormrod's results were lower than predicted by theory by a factor of 3, although corrections to his analysis, which include the effects of the applied magnetic field, tend to reduce the discrepancy somewhat.

Another energy-loss experiment with protons (5–10 keV) was performed by Halverson[5] (1968) using a magnetically confined lithium arc plasma. The protons made a number of passes through part of the arc while their guiding centers precessed because of a ∇B drift. The energy spectra

of fast neutral hydrogen atoms resulting from charge exchange were analyzed, and showed an energy loss of (40–60)% of the predicted value. Plasma parameters were electron density, 4×10^{12} cm^{-3}; electron temperature, $\approx 10^4$ °K. A reanalysis by Caby-Eyaud[7] (1970) reduced the discrepancy with theory in this experiment.

An experiment done by Burke[6] (1972) was performed concurrently with the present one. A beam of 2.8-keV protons or 3.3-keV deuterons was neutralized in a charge-exchange cell, and injected across the field lines into a magnetically confined plasma which was the afterglow of a hydrogen discharge. Some of the fast neutral test particles were ionized through charge exchange and began to rotate in the magnetic field, losing energy to the plasma particles. A small number of these were reneutralized at a point in their orbit which permitted them to enter a shielded detector chamber, where they were reionized and energy analyzed. A number of plasma diagnostics were employed to measure a plasma temperature of $\approx 10^4$ °K, and a density of approximately 6×10^{13} cm^{-3}. Burke's measured energy losses were from 3 to 4 times higher than theoretical predictions, depending on whether or not corrections were applied for magnetic field effects.

In contrast with all of the above experiments, the present work utilizes a steady-state equilibrium plasma that is virtually free of electric and magnetic fields. These conditions minimize the difficulties in comparing the experimental results with theory. We report measurements for several values of beam energies, plasma densities, and plasma temperatures.

III. THEORY

This section briefly reviews the different theoretical approaches to the calculation of the energy loss of a test ion in a plasma. Generally, an ion can interchange energy with a plasma via three processes, namely, inelastic collisions with the plasma (or neutral background) particles, elastic collisions, and through plasma collective effects. Only the last two mechanisms are significant for a low-energy beam of ion test particles in a highly ionized plasma. The test particles in a collimated monoenergetic beam undergo numerous uncorrelated successive small-angle collisions with the plasma particles, so that the beam particles emerge with a distribution in direction and energy. In addition, the test particles may exchange energy with the plasma by exciting a plasma oscillation. For general reviews of the theoretical treatment of the energy-loss problem, see Refs. 8 and 9.

Butler and Buckingham[10] treat the energy-loss problem from a direct-collision point of view. They consider a test particle of mass M and charge Ze traveling with velocity $\vec{V}$ in the laboratory system, and making a series of collisions with field particles of mass m and charge ze traveling with velocity $\vec{v}$. Using central-force binary-collision theory and the differential Coulomb scattering cross section, they derive an expression for the average energy change of the test and field particles. Assuming a Maxwellian distribution of field particle velocities, an integration over velocity is performed yielding the total rate of energy change.

Since the Coulomb scattering cross section leads to a divergence at small scattering angles, it is necessary in the averaging of the energy loss over the center-of-mass scattering angle θ to limit the range of angle to $\theta_{\min}\leq\theta\leq\pi$, where $\theta_{\min}$ is a specific minimum scattering angle, corresponding to a maximum impact parameter on the order of the Debye length.[11]

Butler and Buckingham's expression for the energy-loss rate $(dE/dt)_s$ to the sth kind of field particle is

$$\frac{dE}{dt}=\frac{8\sqrt{\pi}\,n_s(Zze^2)^2F(V/v_s)\ln\Lambda}{m_sv_s}\ , \qquad (1)$$

where n_s is the number density of scatterers, the thermal speed v_s of the plasma constituents is $v_s=(2kT/m_s)^{1/2}$, and

$$F(x_s)=\frac{1}{x_s}\int_0^{x_s}e^{-x^2}\,dx-(1+m_s/M)e^{-x_s^2}\ , \qquad (2)$$

where $x_s=V/v_s$, the ratio of the beam speed to the thermal speed of the plasma particles. Equation (3) only takes the form shown for a Maxwellian velocity distribution of the plasma constituents. The total energy loss rate is given by a sum over all plasma constituents, $dE/dt=\sum_s(dE/dt)_s$.

Another widely used approach to the calculation of the energy-loss rate involves the use of the Fokker-Planck equation, first used in this context by Chandrasekhar[12] to describe the motion of a single star in a star cluster. Rather than considering successive individual collisions, the derivation of the Fokker-Planck equation (as given by Chandrasekhar) treats the effect of many simultaneous small-angle collisions additively so as to produce a total vector change in the test-particle's velocity distribution function $f_t(\vec{x},\vec{v},t)$. The test particle, subject to simultaneous small-angle "grazing" collisions with the plasma electrons and ions which lie within its Debye sphere but which are also mostly far beyond the minimum impact parameter, progresses in velocity space

in a random walk manner. This random motion is superimposed on its directed motion. The derivation assumes a Markovian process—that the future evolution of the distribution function depends on current conditions and not on the past history of the system. The Fokker-Planck equation can also be derived[13,14] by treating the test-particle–plasma interaction as a series of successive small-deflection binary collisions, and expanding the collision term of the Boltzmann equation, using the Rutherford scattering cross section.

Using either derivation one is led to a Fokker-Planck equation of the form

$$\left(\frac{\partial f_t}{\partial t}\right)_{\text{collisions}} = \sum_s \left[\sum_i \frac{\partial}{\partial v_i} \left(-D_i f_t + \frac{1}{2} \sum_j \frac{\partial}{\partial v_j} (D_{ij} f_t) \right) \right]_s . \tag{3}$$

The vector $\vec{D}$ is called the "coefficient of dynamic friction," defined such that $D_i = \langle \Delta v_i \rangle$ is the average increment per unit time of the ith component of the test-particle's velocity. Similarly the tensor D_{ij}, often written as $\langle \Delta\vec{v}\,\Delta\vec{v} \rangle$, is called the "diffusion in velocity tensor" and is a measure of the rate of diffusion of $f_t(\vec{x}, \vec{v}, t)$ in velocity space. Higher-order terms such as $\langle \Delta\vec{v}\,\Delta\vec{v}\,\Delta\vec{v} \rangle$, the "nondominant" terms of Chandrasekhar, may be neglected.

Evaluation of the diffusion coefficients D_i and D_{ij} can be simplified by considering the symmetries of the system. For a test-particle beam with an initial δ-function velocity distribution, incident on a isotropic plasma in the absence of external forces, there are only three nonzero independent diffusion coefficients,[13,15] $\langle \Delta v_\parallel \rangle$, $\langle \Delta v_\parallel^2 \rangle$, and $\langle \Delta v_\perp^2 \rangle$. The dynamical friction coefficient $\langle \Delta v_\parallel \rangle$ is the rate at which the test-particle velocity is changing in the initial direction of the beam particles. The two elements of the diffusion-in-velocity tensor represent the average rate of change of $\langle \Delta v^2 \rangle$ in directions parallel and perpendicular to the beam velocity.

The rate of change of the test-particle energy can be expressed in terms of the diffusion coefficients.[15,16] The mass and velocity of the test particle are denoted by M and $\vec{v}$, respectively, and $(\,)_{\text{ave}}$ denotes an average over all interactions with the plasma constituents. The rate of change of the particle energy is

$$\frac{dE}{dt} = \left(\frac{M}{2\Delta t} \left[(\vec{v} + \Delta\vec{v}) \cdot (\vec{v} + \Delta\vec{v}) - v^2 \right] \right)_{\text{ave}} . \tag{4}$$

Rearranging,

$$\frac{dE}{dt} = \tfrac{1}{2} M \left(2\vec{v} \cdot \frac{\Delta\vec{v}}{\Delta t} + \frac{\Delta\vec{v} \cdot \Delta\vec{v}}{\Delta t} \right)_{\text{ave}} . \tag{5}$$

In terms of the nonzero diffusion coefficients, Eq. (5) becomes

$$\frac{dE}{dt} = \tfrac{1}{2} M \left[2v \langle \Delta v_\parallel \rangle + \langle \Delta v_\parallel^2 \rangle + \langle \Delta v_\perp^2 \rangle \right] . \tag{6}$$

This expression for dE/dt has been evaluated by Spitzer[15] and, in a slightly different manner, by Shkarofsky *et al.*[8] Their results are identical to Eq. (1) derived by Butler and Buckingham.[10] May[17] has shown that the two treatments are equivalent provided that the test-particle energy is greater than the energy of the plasma ions and electrons.

An alternative to the use of the collision theory in calculating the effects of a plasma–test-particle interaction is to use the "wave" theory, which treats the plasma as a polarizable medium. The electric field of the charged test particle polarizes the plasma, and the electric field due to the polarization reacts on the test particle to produce a frictional force. In addition the test charge reacts to the electric field produced by correlated density fluctuations (plasma oscillations) in the plasma. The resulting formulation does not require an arbitrary cutoff at the Debye length, which appears naturally.[8] However, to prevent divergences, it is necessary to introduce an arbitrary cutoff at a minimum impact parameter[9,18,19] $b_{\min}$, which is usually taken to be the impact parameter for 90° deflections in the center-of-mass system.

The collision and wave theories are complimentary; the former is assumed to correctly include the dynamics of binary encounters, and the latter to handle collective phenomena properly. A formulation was initially developed by Thompson and Hubbard,[18,20] to continuously join the two theories so that no arbitrary phenomenological cutoffs are necessary. A number of authors have followed with "convergent" plasma kinetic equations,[21] including a series of papers,[21,22] by Kihara, Aono, Itikawa, and co-workers. Generally, such convergent theories have not produced a tractable expression for the energy-loss rate of a test ion over a broad range of velocities, except for a paper by Itikawa and Aono.[23] For a test ion of mass M, velocity V, and charge q, traversing an infinite homogeneous plasma at temperature T and density n_s, the energy-loss rate of the particle is given by

$$\frac{dE}{dt} = 4\pi q^2 \sum_{s=1}^{2} \frac{n_s e_s^2}{m_s v_s} \left[F_s(V/v_s) \ln \left(\frac{4\mu_s kT\lambda_s}{\gamma |e_s q_s| m_s} \right) + G(V/v_s) \right] , \tag{7}$$

where

$$F_s(x_s) = \frac{2}{\sqrt{\pi}} \left[\int_0^1 e^{-u x_s^2} \, du - \left(1 + \frac{m_s}{M} \right) e^{-x_s^2} \right] . \tag{8}$$

An expression equivalent to Eq. (7) has also been given by Perkins.[24] Again the subscripts label the various plasma constituents with m_s, v_s, and e_s, the same as defined earlier. The other quantities in Eq. (7) are the reduced mass

$$\mu_s = m_s M/(m_s + M) ,$$

the Debye Length

$$\lambda_s = (kT/4\pi n_s e_s^2)^{1/2} ,$$

Boltzmann's constant k, and Euler's constant

$$\ln\gamma = 0.5777\ldots .$$

$G(V/v_s)$ represents the dependence of the Coulomb logarithm on the velocity of the test particle. Graphs of the function $G(V/v_s)$ for a two-component singly ionized plasma were presented by Itikawa and Aono.[23] Equation (7) does not include quantum-mechanical effects.

In spite of the diversity of theoretical approaches, all the expressions for the energy loss agree to within about 20% in the range of parameters involved in this study. On the other hand as already mentioned the few experiments that have been done with ion beams give energy losses that range from substantially higher to several times lower than that predicted by the theory.

The quantity which is measured experimentally for a given beam energy, plasma temperature, and plasma density is the total energy loss of the beam, ΔE. To relate ΔE to expressions for the energy-loss rate dE/dt [Eq. (7) or (1)], the theoretical expression must be multiplied by Δt, the transit time of the beam ion through the plasma. The transit time is set equal to L/V, where L is the length of the plasma and V is the speed of the beam ion. This is a good approximation when the magnitude of the energy loss is small compared to the beam energy (i.e., $\Delta E/E \ll 1$). Both theory and experiment give values of $\Delta E/E$ which are substantially smaller than unity, supporting this approximation. The dependence of the energy-loss rate on test-particle speed and plasma constituents is graphically illustrated in Fig. 1. This shows the calculated energy loss per cm of a Cs^+ beam as a function of x_e, the ratio of beam speed to the plasma electron thermal speed. Equation (1) has been used, and a cesium thermal equilibrium plasma at 2500 °K with a density of 2×10^{11} cm^{-3} has been assumed. Two peaks are seen, one due to electrons, the other due to singly charged cesium ions. The peak near $x_e = 0.003$ results primarily from loss to plasma ions with its center near the point where the beam speed would equal the thermal ion speed, an energy of about 0.2 eV. Note that an energy gain would result if the beam ions could be injected at subthermal energies. The peak at $x_e \cong 1$ results primarily from the energy loss to electrons, and is the dominant loss mechanism in our experiment. In particular, for our cesium plasma, the theory predicts the energy loss to ions for a test-particle beam of cesium ions will be approximately 0.3 to 0.05 the energy loss to electrons for beam energies of 35–150 eV. For a test-particle beam of lithium ions in the same energy range the energy loss is almost completely due to electrons. Noted on the graph are the regions investigated in the present measurements as well as the x_e values used in other

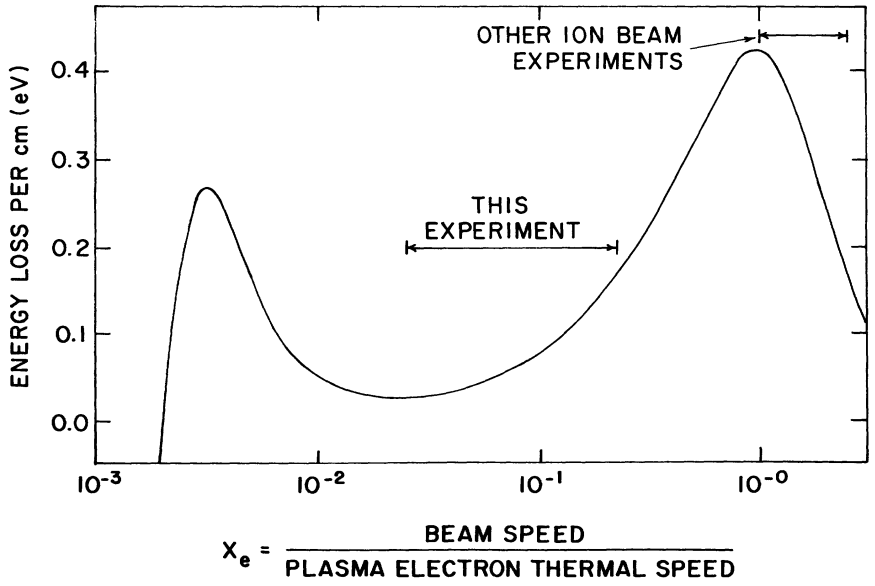

FIG. 1. Energy loss per centimeter of a cesium ion beam traversing a 2500 °K cesium plasma with a density of 2×10^{11} cm^{-3}. The abcissa is the ion beam speed divided by the electron thermal speed, or x_e. The range of this parameter investigated by this experiment and other ion beam experiments is shown.

experiments. The general shape of this curve is fairly insensitive to plasma temperature. Thus previous experiments carried out at considerably different temperatures from the present ones can be qualitatively compared on this graph.

Our experiment actually measures the part of the energy loss associated with $\langle \Delta v_{\parallel} \rangle$, while Eqs. (1) and (7) give the total energy loss. We use Eq. (7) for comparison with our data because it has no arbitrary parameters associated with it, but it should overestimate the energy loss as measured by us because it includes the energy loss due to the diffusion coefficients [see Eq. (6)]. Using the expressions given by Spitzer[15] for $\langle \Delta v_{\parallel} \rangle$ and the diffusion coefficients, we estimate the error to be 10% for our 35-eV Cs^+ beam, and considerably smaller for all other data.

IV. THE PLASMA

As the type of plasma used in this investigation is not one of the more familiar varieties, we include a brief review. If a fixed number of atoms with density n_t and ionization energy Φ is placed within a isothermal enclosure whose walls are maintained at a temperature T, a plasma is formed whose electron density n_e, ion density n_p, and neutral density n_0 are related by the Saha equation,[25]

$$\frac{n_e n_0}{n_0} = \frac{2g'}{g}\left(\frac{2\pi m_e kT}{h^2}\right)^{3/2} e^{-\Phi/kT}, \qquad (9)$$

where m_e is the mass of the electron, and k and h are Boltzmann's and Planck's constants, respectively. The ratio of the statistical weights of the ionized and neutral atoms is g'/g ($=\frac{1}{2}$ for alkali metals). Under steady-state conditions (and for single ionization) $n_p = n_e =$ "plasma density." The fractional ionization $I_f = n_p/n_t$, where $n_t = n_p + n_0$, increases with T for constant n_t and decreases at constant T for increasing n_t. On the other hand, n_p increases monotonically for constant T and increasing n_t. The cross-hatched region of Fig. 2 depicts the area under investigation in the present measurements while Table I lists some of the typical parameters for our plasma at the operating conditions.

Thus, an equilibrium laboratory plasma can be produced using an alkali element with a low ionization potential in a suitable refractory enclosure. This idea was first suggested by Dreicer[26] and several versions of such a plasma device have been constructed. All the designs,[27-30] however, suffer from one or more of the following shortcomings: (i) The temperature of the enclosure is not uniformly maintained over long periods of time; (ii) The useful lifetime of the device is severely limited at high temperature (~2500 °K); (iii) There is no way of allowing an external particle beam to interact with the plasma. The plasma source used in the current experiment, utilizing cesium vapor in a tantalum enclosure, does not suffer from the above problems.

With the size plasma container, temperatures, and densities used in this experiment, the primary mechanism for ionizing and thermalizing the cesium atoms is collisions with the walls. From the ratio of the wall area to the area of the holes in the plasma chamber, it is calculated that the plasma particles on the average must make

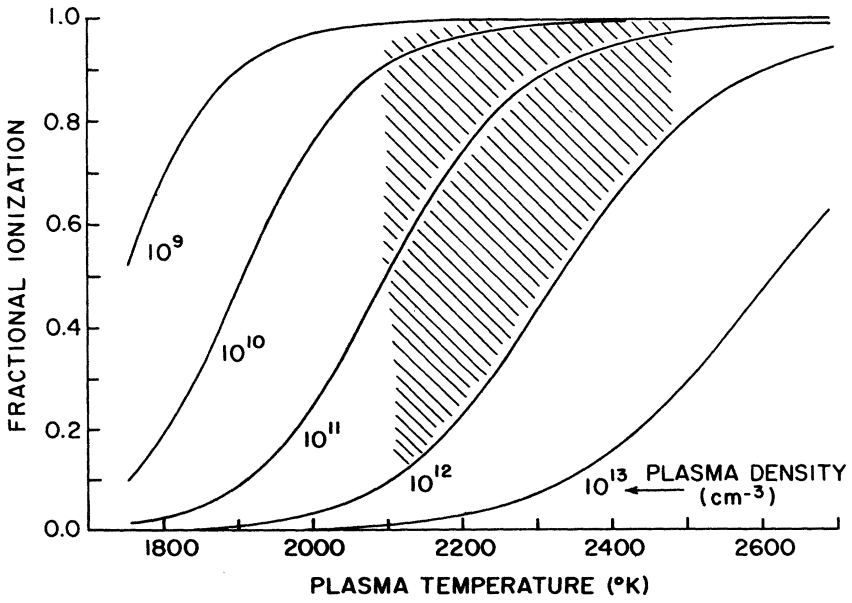

FIG. 2. Fractional ionization of cesium as a function of temperature as predicted by the Saha equation. Each curve is for a given plasma density.

TABLE I. Typical plasma parameters.

Temperature (°K)	2500	2500	2100	2100
Electron/ion density (particles/cm^3)	10^{10}	10^{12}	3×10^{11}	10^{10}
Fractional ionization	0.998	0.826	0.29	0.923
Density of neutral background (atoms/cm^3)	2×10^{7}	2.1×10^{11}	7.5×10^{11}	8.3×10^{8}
Debye length (cm)	3.4×10^{-3}	3.4×10^{-4}	5.8×10^{-4}	10^{-3}
Number of particles in a Debye sphere	3400	340	484	838

several hundred collisions with the walls before escaping from the plasma region. Even if a particular relaxation mechanism required 5 or 10 collisions with the walls, thermal equilibrium should be closely established and the Saha equation should give a good description of the plasma. It is interesting to note that the Saha equation does not depend on the properties of the wall, but for a container with exit holes it is necessary to use a suitably high-work-function material for the wall so that the probability of ionization on a single wall collision is quite high. Cesium with an ionization potential of 3.893 eV and tantalum with a work function of 4.12 eV fulfill this criterion very adequately.

V. APPARATUS

An over-all schematic of the experiment (not to scale) is shown in Fig. 3. The ion beam originates at the cathode; it is extracted, decelerated, and collimated by electrostatic lenses and deflected onto the main axis by the first set of deflection plates. After passing through a hole in the water-cooled ion-gun-shield flange, the beam may be slightly trimmed in direction by a second set of deflection plates. The beam is further collimated as it enters the plasma cylinder by the plasma-cylinder entrance aperture. The ion beam passes through the plasma cylinder and the third set of deflection plates and into the detector. A cesium oven supplies alkali vapor to make up for the losses from the diagnostic holes in the plasma chamber. The neutral density in the plasma is measured with a surface ionization detector, and the temperature is measured with an optical pyrometer. The following paragraphs describe these components in more detail.

Figure 4, with the exception of the cesium oven, is a cross section of the plasma confinement and heating system. The cesium oven has been rotated by 45° so it could be included in the diagram. The plasma is contained in a 1-mil wall tantalum tube 1.905 cm in diameter and 12.57 cm long. A series of disks spotwelded into the tube confine the plasma and provide heat shielding. Holes in the center of the disks serve as apertures for the ion beam. The two disks actually containing the plasma are 7.5 cm apart when hot. The beam entrance and

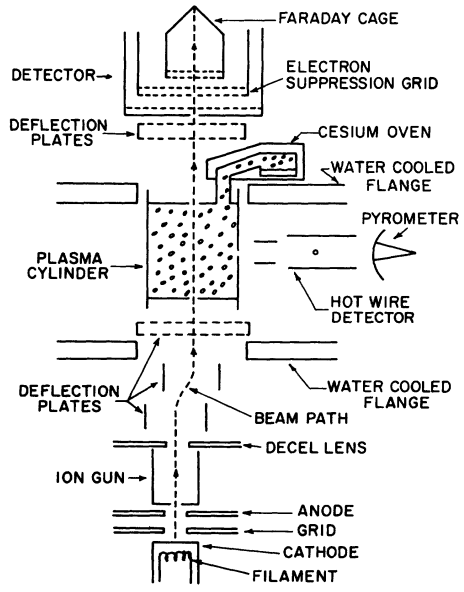

FIG. 3. Schematic of the apparatus showing the arrangement of the components. It is not to scale.

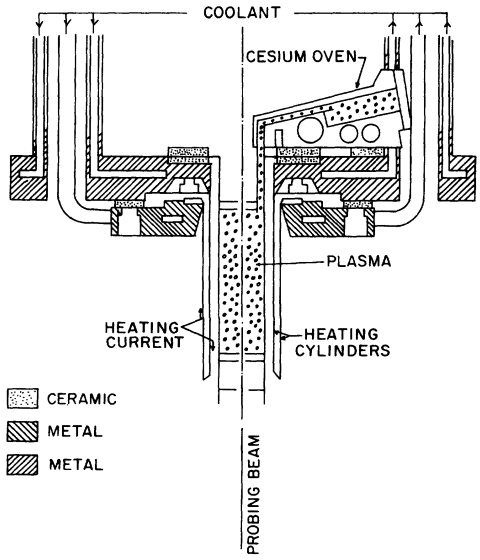

FIG. 4. Detailed drawing, to scale, showing the plasma chamber, heating elements, and support structure.

exit holes to the plasma region are 0.170 and 0.318 cm in diameter, respectively. Cesium is fed from a nickel oven into the plasma cylinder by a tube of rolled up tantalum foil. The oven has a noninductive heater, cooling coils that allow it to be quenched quickly, and several chromel-alumel thermocouples for temperature monitoring. A temperature controller stabilizes the oven temperature to within a fraction of a degree. The highest oven temperature used was 140 °C.

Two coaxial, tungsten-foil cylinders of 1-mil wall thickness are used as a resistive heating element to control the temperature of the plasma. The two cylinders are spotwelded together at their lower ends. The upper ends are attached to two electrically isolated water-cooled flanges. The heating current can thus be passed down one cylinder and back up the other almost entirely eliminating magnetic fields due to the relatively large heating current. The present design for the plasma-cylinder heating element is the result of much experimentation. Previous versions using tantalum foil have operated satisfactorily at temperatures below 2100 °K[30] but failed quickly at higher temperatures. Thus the great increase in operating life afforded by using tungsten cylinders far outweighs the difficulties involved in fabricating the tungsten cylinders. The present freely hung design minimizes stresses on the cylinders due to thermal expansion and contraction. A smaller temperature differential between the heating and plasma cylinder was observed with this design than with a design in which the heating element was comprised of a single cylinder. The negative terminal of the heating-element power supply is grounded so as to suppress electron emission. The entire length of the heating element is thus positive with respect to the surrounding grounded components. Not shown, but surrounding the heating element, are two cylindrical tantalum heat shields attached to the water-cooled flange.

The water-cooled flanges from which the plasma, heating, and shielding cylinders are suspended, are supported by two sets of concentric tubes which carry coolant (water) and dc current for the heating element. Each set of tubes carries half the heating current in a coaxial manner to reduce stray magnetic fields. All the currents are matched to within 0.2 A by parallel rheostats. A current of 250 A at 16.8 V is necessary to heat the plasma cylinder to around 2500 °K.

The temperature of the plasma cylinder is determined by measuring the temperature of the blackbody radiation from a small hole (0.160 cm in diameter) in the side of the cylinder with an optical pyrometer. The pyrometer hole is located approximately midway between the two caps defining the plasma region. The temperature profile along the length of the plasma cylinder has been examined on an apparatus similar to the present one, but with inferior heat shielding. It is estimated (taking into account the improved heat shielding of the present system) that the temperature variation of the plasma region is less than 20 °K at a temperature of 2500 °K.

The density of neutral cesium atoms in the plasma cylinder is measured by monitoring the efflux of neutral cesium from the pyrometer hole which impinges upon a modified Langmuir-Taylor[31,32] surface ionization detector. A schematic of the hot-wire detector and electronics is shown in Fig. 5. The detector surface is a 2.5-cm length of 0.025-cm-diam tungsten wire, mounted vertically along a diameter at the center of 3.8-cm long stainless-steel collector. A positive bias is applied to the wire and a negative bias to the collector. A battery-powered electrometer, floated at the collector potential is used to monitor the ion current.

In contrast to the usual design of many hot-wire detectors, the rear of the collector is left open, in order to allow optical pyrometer measurements of the plasma-cylinder temperature through this aperture. The hot-wire detector is operated in a mode such that the collected ion current is independent of bias voltage, ensuring close to 100% collection efficiency. A set of electrostatic deflection plates are positioned directly in front of the collector to sweep out charged particles emanating from the plasma region. A beam flag is positioned in front of the deflection plates. The neutral current due to atoms effusing from the pyrometer hole is obtained by subtracting the background detector current (less than a few times 10^{-12} A) with the beam flag closed from the signal when the beam flag is open (10^{-11}–10^{-9} A).

The hot wire is usually operated at a temperature (measured by the optical pyrometer with no emissivity corrections) of 1000–1300 °K, a regime

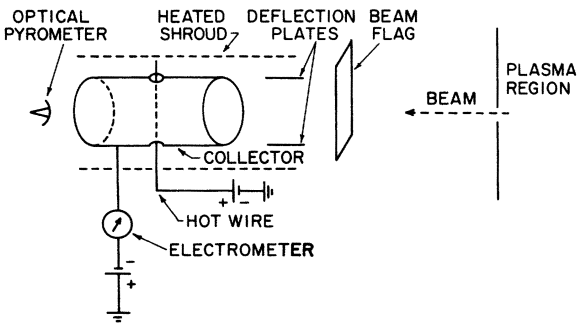

FIG. 5. Schematic drawing, not to scale, showing the hot wire and beam flag.

where the ionization efficiency[33] for cesium is close to 100% and where the detected ion current does not change as the temperature of the wire is varied.

The ion gun located below the bottom water-cooled flange consists of an ion source, extraction and focusing electrodes, and a set of deflection plates to offset the beam. The source of alkali-metal beam ions (Cs^+ or Li^+) is a commercial alkali-ion dispenser cathode.[34] A Soa[35,36] lens is used as the extraction stage and cylindrical lenses are used for acceleration and deceleration. The gun was constructed of a series of stainless-steel cylinders insulated from each other by small sapphire balls.

In early testing of the apparatus, neutral atoms effusing from the plasma cylinder traveled down the ion gun axis, ionized on the hot cathode, and joined the beam. Since it was deemed undesirable to have the beam intensity thus partially controlled by the plasma density, the gun axis was displaced with respect to the final beam axis. Two pairs of deflection plates were installed at the gun exit to deflect the beam back onto the main beam axis. A small Faraday cup was also installed in this region so that the beam intensity could be monitored before passage into the plasma region.

A schematic version of the ion beam detector is shown at the top of Fig. 3. The detector is constructed following a design of Stephanakis and Bennett.[37] Three concentric cylinders, each capped with a pair of interconnected mesh grids (0.001-in. tungsten, 92% transparent) to minimize electric field interpenetration among adjacent regions of the detector and electrically isolated from each other, comprise the detector. The outermost cylinder is grounded to serve as an electrostatic shield and to keep stray particles from entering the detector region.

The second or intermediate cylinder is needed only for the pair of grids at its end. These can be used to apply a retarding potential for energy analysis of the incoming beam (the "filter mode"),[38] or to suppress charged particles of sign opposite to the ones being detected (the "classical" mode). In the latter mode, most often used by us, the retarding potential is applied directly to the Faraday cup. In general, the choice of operating mode depends upon the width of the energy distribution obtained under identical beam conditions. The suppression cylinder is attached to the shield cylinder with an Aremcolox ring.

The central cylinder is used as the ion collector. It is usually recommended that the cup be made at least ten times as deep as the diameter of the opening in order to achieve 95% collection efficiency.[39] In addition, the back of the cup should be an acute angle. The actual diameter-to-length ratio of our cup is 8.25. The cup is also half-filled with mesh to increase collection efficiency. A special effort is made to maximize the impedance between the cup and any other conductors (including ground). It is mounted on a 0.343-cm-thick BeO disk which is held with a retaining ring; the lead to the second cylinder passes through a hole in this disk without touching it. The resistance between the cup and the second cylinder suppressor, or to ground, is measured to be greater than 10^{13} Ω at 175 °C.

To ensure a constant work function over the entire detector surface, and to minimize contact potential differences, all metal parts were coated with Dag dispersion. To further shield the detector from stray charged particles, a grounded shield was installed around the detector. With this additional shield in place, the ion beam off, and the detector set to suppress both plasma electrons and ions, less than 10^{-13} A of residual current was observed at the detector.

For the plasma to be at least nominally free from external electric and magnetic fields, it is necessary to provide adequate shielding, and to minimize the introduction of disturbing fields within this shielded region. The plasma is electrostatically shielded by grounding the plasma container. The main vacuum chamber is also partially magnetically shielded by several layers of Netic and Conetic foil wound around the outside of the chamber. Presence of the pump stack (adapter, valve, trap, and pump—all nonmagnetic stainless steel) and the main cover flange, as well as the side ports, prevented complete magnetic shielding of the chamber. All internal heaters are noninductively wound, and direct current is used whenever possible to minimize 60-Hz pickup.

The entire assembly described above is contained in a stainless-steel vacuum system. This system is pumped with a 6-in. oil diffusion pump equipped with a zeolite baffle. For additional pumping, a small liquid-nitrogen trap is mounted on one flange and for thermal isolation a large water-cooled baffle almost completely surrounds the plasma assembly. With the plasma chamber at 2500 °K, pressures of the order of 4×10^{-7} torr are obtained.

VI. EXPERIMENTAL PROCEDURE

The ion beam at energy E is passed through the plasma at some temperature T and electron density n_e. The beam enters the detector which is normally operated in the "classical mode," with the (positive) retarding potential applied to the Faraday cup, and the suppressor grid held at a negative potential to exclude all ambient electrons. An electrometer floated at the retarding potential

V_0, is used to measure the current to the Faraday cup. In order to sweep the retarding potential a few volts about the value set by the retarding-potential power supply, this supply is floated on a linear-symmetric triangle voltage wave of height $\pm\Delta V$ about zero. The retarding voltage on the Faraday cup is thus swept $\pm\Delta V$ about V_0. The output signal from the electrometer and the triangular wave voltage are both fed into voltage-to-frequency converters and then to two of the multiscaling inputs of a multichannel analyzer, operated in a multiple input, zero dead time, simultaneous multiscaling mode. In this manner both the detector current and the retarding voltage (relative to V_0) can be recorded simultaneously as a function of time.

It is necessary to get a "zero" density measurement for calibration purposes. The plasma cylinder is brought to operating temperature (2100–2500 °K). The cesium oven is kept cold (~10 °C). The system is baked at this temperature until a negligible density is indicated by the surface ionization detector. This typically takes on the order of an hour after reaching operating temperature. This is taken as the zero density measurement corresponding to zero energy loss.

A data run consists of a number of plasma density cycles. During each cycle, beam current-retarding voltage curves at each beam energy are taken with the cesium oven cold. The oven is then heated, in a number of preset steps, until the maximum plasma density is reached. At each step a set of current-voltage curves for different beam energies is taken. The oven temperature is then stepped downward, again taking current-voltage curves at each step.

Data were taken in this manner because the beam energy is more easily varied than plasma density. Variation of the plasma density requires at least 15 min for the cesium oven to reach equilibrium. When the plasma is quenched, by passing cold water through the oven cooling tubes to freeze the cesium, an additional 30 min must be allowed for the residual cesium to be pumped out of the cylinder. When the plasma-cylinder temperature is changed, even more time is required for complete thermal equilibrium to obtain.

VII. EXPERIMENTAL UNCERTAINTIES

In addition to the interaction of the plasma with the beam ions, there are two other competing mechanisms that could measurably affect the energy of the test ions. These processes are both dependent on the density of neutral atoms within the plasma, and act to produce opposite effects. The first is energy loss in the lab system due to elastic scattering in the center-of-mass system with the neutral atoms in the plasma. The other is a reduction of the effective path length of the beam through the plasma via a double charge-transfer process, resulting in a decreased energy loss. It is shown in Appendix A that the contribution to the energy loss of the Cs^+ beam ions due to elastic scattering with the neutral Cs background in the plasma container may be neglected at our operating conditions.

For a plasma with a nonzero neutral background, there is a finite probability that a beam ion will enter the plasma, charge transfer with a neutral atom, and travel some distance through the plasma before undergoing a second charge transfer with a plasma ion, and emerge from the interaction region as an ion. This double charge-transfer process reduces the effective path length for ion-plasma energy-loss interaction, since the fast neutral particle loses essentially no energy to the plasma.

The average distance L_1 that the beam particle travels as an ion through the plasma is

$$L_1 = (LW + SQ)/(W + Q) ,$$

where L is the total plasma length, S is the average distance traversed as an ion by a beam particle that undergoes a double charge-exchange process, W is the probability that an ion travels through the entire plasma as an ion, and Q is the probability that an ion undergoes as a double charge-exchange process. The full expression for L_1 is derived in Appendix B. The ratio L_1/L is the correction factor that must be applied to the calculated energy loss to compare it to our measurements. For the maximum neutral densities encountered in this experiment and a Cs^+ ion beam, $L_1/L > 0.985$. For a Li^+ beam, L_1/L is effectively unity because the nonresonant charge-transfer cross sections[40–42] are considerably smaller than the resonant charge-transfer cross sections at these energies. Therefore, the reduction of the effective path length through a double charge-exchange process is not significant in the present measurements.

Measurement of a change in the transmitted ion-beam energy requires precision in determining an energy difference between an unattenuated and an attenuated ion beam, rather than an accurate measurement of the actual ion-beam energy. Consequently, the effects of any thermal potentials or contact potentials present along the beam path may be ignored, provided that they do not change over the measurement period. Certain precautions were taken in an attempt to minimize the variation of such potentials on a short-term (24–36 h) basis. The ion-beam source and detector were continu-

ously maintained at high enough temperatures (~175 °C) to prevent deposition of contaminants on their surfaces. Detector surfaces were also carbon coated to minimize variations in contact potentials. No beam measurements were made without the plasma source having been at operating temperature long enough for the apparatus to thermally stabilize; additional stabilization time was allowed when the cylinder temperature was changed.

It should be noted that the primary source of uncertainty of this type is probably a surface contamination when cesium is introduced into the plasma chamber. If so, the only surfaces which could affect the measurement of the beam energy are the cathode, which is shielded from the line of sight of the plasma chamber, and the Faraday-cup beam collector, which is moderately far away and is heated. Thus, uncertainties due to time-varying surface effects are considered to be minimal.

Generally, when a plasma contacts an external surface, a plasma sheath whose dimensions are on the order of the Debye length, is formed between the two. The sign and magnitude of the potential drop across the sheath is a function of the plasma and surface parameters as well as the geometry of the system. For our plasma, the sheath may be positive or negative depending on the plasma temperature and density[43] and the potential is on the order of a few tenths of a volt. The effects of the sheath on our energy-loss measurements are minimal. Since the plasma potential may be slightly different from that of its grounded container, the beam energy in the plasma may vary slightly from the energy measured at the detector. But, the value of the beam energy as measured at the detector is independent of its passage through the plasma sheaths since energy lost or gained on entering the plasma through the sheath would be gained or lost on exiting through the sheath.

The plasma sheath may also have a lens effect on the beam at the entrance and exit apertures of the plasma region, and attenuation of the beam can be caused by defocusing at the apertures as well as by bonafide plasma effects. However, defocusing will lead only to a loss of intensity and not to an error in energy loss in the forward direction.

If the detector system has a time constant, the energy sweep speed of the detector will cause distortion in the effective shape of the measured energy distribution.[44] Only difference measurements are done in the present experiment, so that both the unattenuated and attenuated beams are subject to the same distortion. Any uncertainties due to sweep speed are therefore at most of second order and can be neglected.

Errors in measuring the energy shift due to repeatability and resolution of the voltmeters used to measure the cathode and retarding potentials is on the order of a few mV. The multichannel analyzer introduces an uncertainty in energy resolution of ± 1 channel, or an average of ±0.026 V for the cesium beam data, and ±0.019 V for the lithium beam data. Estimated total uncertainties in the measurement of the energy loss vary from 0.027 to 0.05 eV with some typical values shown in Figs. 7–11.

The plasma density is calculated from the measured values of the neutral density and the temperature by using the Saha equation, Eq. (9). From this equation, the relative uncertainty in the plasma density is

$$\frac{\Delta n_p}{n_p} = \frac{1}{2}\frac{\Delta n_a}{n_a} + \left(\frac{3}{2} + \frac{\Phi}{kT}\right)\frac{\Delta T}{T}$$

$$= 0.5\frac{\Delta n_a}{n_a} + 0.0086\Delta T \ , \qquad (10)$$

where Δn_a and ΔT represent the uncertainties in the neutral density and the temperature measurements, and the last expression on the right assumes $T = 2100\,^{\circ}\mathrm{K}$. We estimate, from uncertainties in dimensions, temperature, and current measurement, that $\Delta n_a = \pm 0.05$. The error in measuring T, due to window losses and instrumental factors, is estimated to be $\pm 20\,^{\circ}\mathrm{K}$ at $2100\,^{\circ}\mathrm{K}$. Putting these values in Eq. (10) the total relative uncertainty in the plasma density at $2100\,^{\circ}\mathrm{K}$ is $\Delta n_p/n_p = \pm 0.20$.

VIII. DATA ANALYSIS AND DATA

The beam currents stored in 400 channels of the multichannel analyzer, along with the measured differences of retarding voltage per channel, enable a retarding-potential curve to be constructed. The derivative of this curve, which is the energy distribution of the beam, is obtained in two ways. In the first, the smoothing function of the analyzer is used three times, and then the differentiation function is used once. In the second, a high-degree polynomial is fitted to the digital data using an orthogonal least-squares technique. The set of points calculated from the polynomial is then differentiated using a three-point formula in which the derivative at channel $n \propto$ (contents of channel $n+1$) − (contents of channel $n-1$). It is important to note that the fitted polynomial itself cannot be differentiated because it generally will oscillate between fitted points, so that although the fit to the data may be excellent, there is no correlation between the derivative of the polynomial and that of the I-V curve.

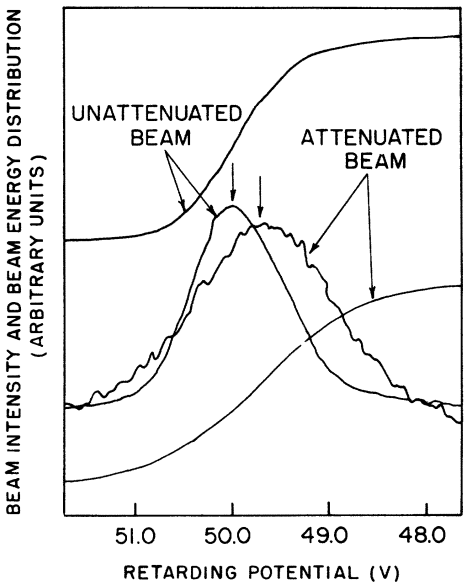

FIG. 6. Retarding-potential curve and its derivative, the energy distribution, for a 50-eV cesium ion beam traversing a 2100 °K cesium plasma. The plasma densities for the unattenuated and attenuated beams were 1.66×10^{10} and 3.09×10^{11} cm^{-3}, respectively. The arrows show the points determined to be maxima.

The derivative of the smoothed *I-V* curve is insensitive to the degree of the polynomial within a range of 15–45. This can be determined empirically by observing the difference in peak position and full width at half-maximum (FWHM) for polynomials of different degree fitted to many test data sets. All the data presented using this method are smoothed using a polynomial of degree 20.

Figure 6 shows the raw data from which a single energy-loss point is determined. It is for a 50-eV Cs^+ beam passing through a 2100 °K plasma. Both the beam intensity and its derivative, the beam energy distribution, are shown as a function of the retarding-potential voltage. The plasma density for the unattenuated and attenuated beams are 1.66×10^{10} and 3.09×10^{11} cm^{-3}, respectively. The curves are tracings made from *x-y* graphs produced by the multichannel analyzer, whose differentiation function was used to produce the energy distribution curves. The two arrows, which are located at 50.021 and 49.666 eV, are the peaks of the curves as determined by computer analysis. As is to be expected, the width of the energy distribution is narrower for the unattenuated than for the attenuated beam, and the full widths at half-maxima are 1.155 and 1.849 eV, respectively.

The data are presented graphically in Figs. 7–11, each showing the variation in observed energy loss (ordinate) with increasing plasma density (abscissa). Each graph shows all the data points taken at a particular beam energy and plasma temperature, with a different symbol being used (square, triangle, etc.) for each run. The solid lines are the predictions of theory, and are very close to being straight lines. The dashed straight lines are least-square fits to the data, with the lines not being required to go through the origin.

The line fitted to the Cs^+ data at 2100 °K (Figs. 7–9) is generally in very good agreement with the theoretical energy loss predicted by Eq. (7) while the scatter of the data points provides a measure of the statistical uncertainty. The 50-eV data shown in Fig. 7 represent the largest number of

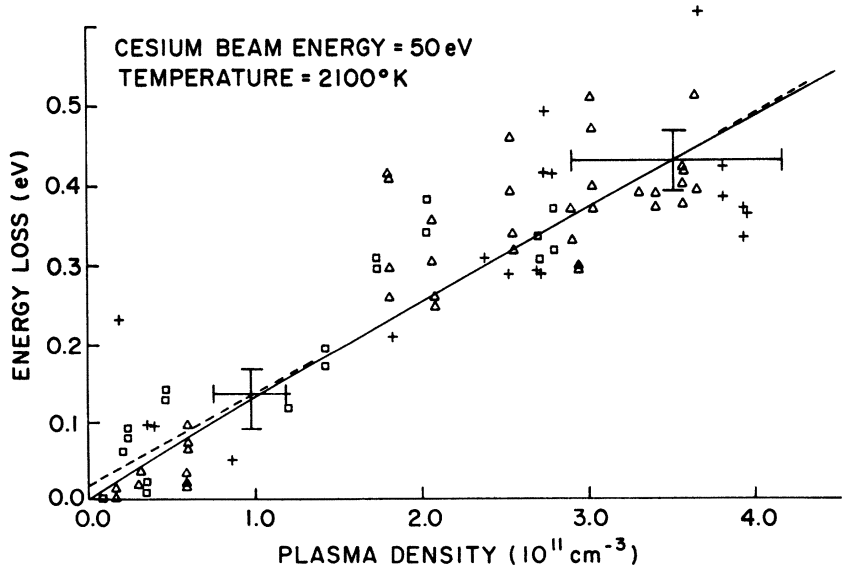

FIG. 7. Energy loss of a 50-eV cesium ion beam traversing a 2100 °K plasma as a function of the plasma density.

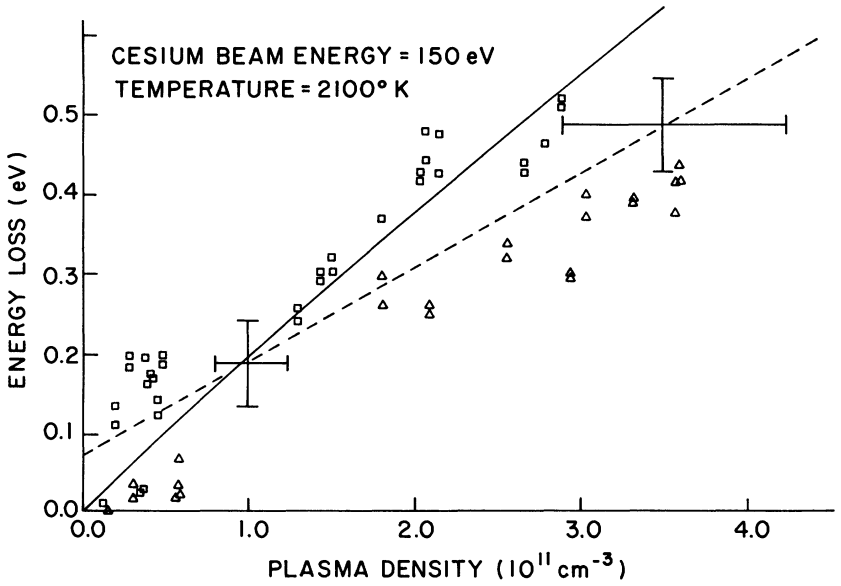

FIG. 8. Energy loss of 150-eV cesium ion beam traversing a 2100 °K plasma as a function of plasma density.

data points, and their fit to the theoretical curve is excellent. At 150 eV, presented in Fig. 8, the data points follow two readily discernable trends, corresponding to runs *A* and *C*. In this case the average falls somewhat below the theory, though run *A* corresponds closely to the theoretical prediction. The signal-to-noise ratio was poorest at 35 eV, and this is evidenced by the large scatter shown on Fig. 9. Beam attenuation varied inversely with energy, so that the 35-eV data was most susceptible to short-term fluctuations in the plasma density.

The results of the single run taken at 2500 °K with a 150-eV Cs^+ beam are shown in Fig. 10. The fitted line is very nearly parallel to the theoretical curve, but is displaced, suggesting the presence of a systematic error in the density or energy loss measurements which was not significant at 2100 °K. For example, due to the high temperature being used here, there could have been appreciable non-alkali plasma density (e.g., tantalum) which would not have registered on the hot wire, and would have produced an energy loss even at zero alkali plasma density.

Figure 11 shows the energy loss of a 150-eV Li^+ beam in a 2400 °K plasma. The agreement with theory is seen to be excellent. Not shown are some energy loss values of a 150-eV Li^+ beam in a 2134 °K plasma. The agreement with theory is good up to a plasma density of about 2×10^{11} cm^{-3}, but for densities higher than this, start to fall below the theoretical value. This discrepancy is not

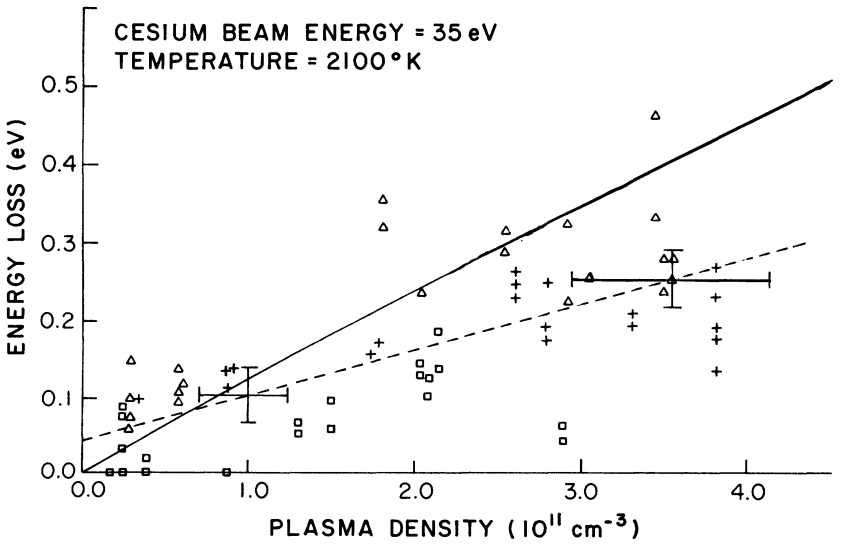

FIG. 9. Energy loss of a 35-eV cesium ion beam traversing a 2100 °K plasma as a function of plasma density.

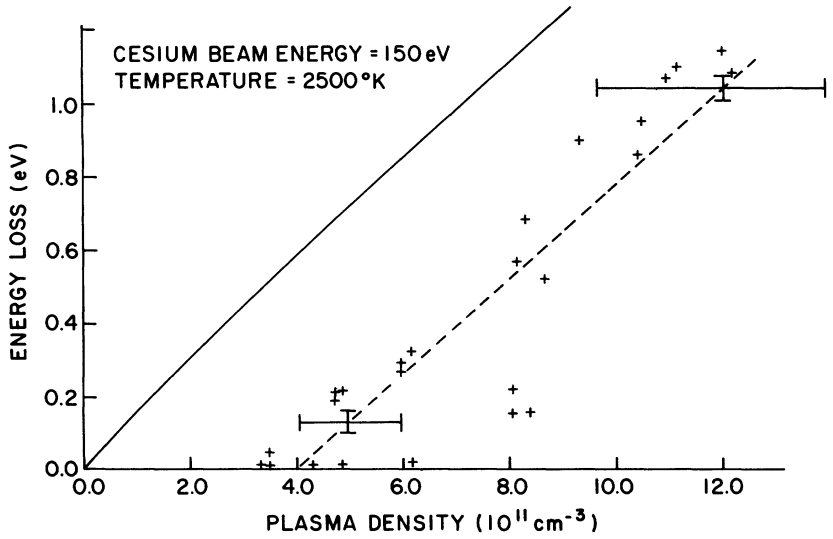

FIG. 10. Energy loss of a 150-eV cesium ion beam traversing a 2500 °K plasma as a function of plasma density.

understood at this time. Disintegration of the plasma chamber due to attack by the Li prevented further immediate checks.

IX. CONCLUSIONS

Apart from the higher-density measurements at 2134 °K with the Li^+ beam, the agreement between our results and the predictions of theory is uniformly good, considering the experimental uncertainties. We conclude that a high degree of confidence can be placed in the theory for the range of the x_e parameter (ratio of beam speed to plasma electron thermal speed) under consideration. As this is the only experiment done at these particular x_e values, the question arises as to whether the disagreement obtained by other investigators at x_e around 1 is due to experimental difficulties or a breakdown of the theory in this range. Nonadiabatic dynamic effects will, of course, become more pronounced at higher x_e. We are now extending our measurements to this energy range in order to investigate this question.

Another unknown is the effect of the magnetic field, used in most of the other experiments, on the energy-loss rate. Theoretical estimates[45] indicate that the magnetic fields used should not have a substantial effect. On the other hand, there has been no experimental verification of this. Ideally, one would like to have a plasma on which a magnetic field could be applied externally without perturbing the plasma significantly, and measure the energy loss with and without the field. We are currently investigating the feasibility of doing such measurements on our apparatus.

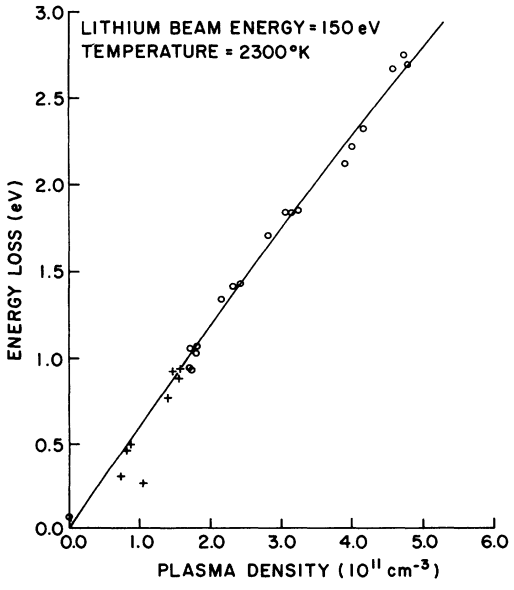

FIG. 11. Energy loss of a 150-eV lithium ion beam traversing a 2300 °K plasma as a function of plasma density.

APPENDIX A: ENERGY LOSS CAUSED BY ELASTIC ION-ATOM COLLISIONS

A plasma ion would lose energy to the background neutral atoms in the same way it interacts with the plasma particles, namely, through a large number of small-angle collisions. Therefore, we will examine the Cs-ion–Cs-atom cross section for scattering through an angle greater than a small angle θ_s much less than the angular resolving power of the ion detector.

Assuming spherically symmetric ions and atoms, at separations larger than the atomic and ionic dimensions, the interaction between an atom and an ion is that of a point charge on an induced di-

pole.[46] The force is attractive, and is given by

$$F_{i-a}=2\alpha e^2/r^5 \tag{A1}$$

for a singly charged ion, where e is the electron charge, r the interparticle separation, and α is the dc electric polarizability of the atom ($=5.96\times10^{-23}$ cm^3 for Cs).[47] The corresponding mutual potential energy of the ion and atom is

$$V_{i-a}=-\alpha e^2/2r^4 . \tag{A2}$$

For small scattering angles, the relation between the impact parameter b and the scattering angle θ, for the potential in Eq. (13), is given by Kennard's small-angle approximation[48]

$$b=1.95\times10^{-8}(\alpha'/V\theta)^{1/4}\ \text{cm}\ , \tag{A3}$$

where θ is measured in radians, α' is the electric polarizability in cubic angstroms, and V is the energy of the beam ions in electron volts. The corresponding cross section for scattering into an angle θ or greater is

$$\sigma(\theta)=\pi b^2=1.19\times10^{-15}(\alpha'/V\theta)^{1/2} . \tag{A4}$$

The cross section $\sigma(\theta)$ for $\theta=10^{-3}$ rad (≈ 20 times smaller than the angular resolution of our detector) is approximately 5×10^{-14} cm^2 for 35-eV beam ions. The mean free path for such a collision at the maximum neutral density encountered in this experiment, approximately 10^{12} cm^{-3}, is 20 cm—almost 3 times longer than the plasma dimension.

In contrast, for small-angle Coulomb collisions we have[8]

$$b=2b_0/\theta\ , \tag{A5}$$

where b_0 is the 90° impact parameter. Using $b_0\approx10^{-8}$ cm, and $\theta=10^{-3}$ rad, the cross section for scattering through angles greater than θ is

$$\pi b^2\cong 12b_0/\theta^2=1.2\times10^{-9}\ \text{cm}^2\ , \tag{A6}$$

over four orders of magnitude larger.

APPENDIX B: DERIVATION OF THE CHARGE-TRANSFER CORRECTION FACTOR

The scattering path length of an ion traversing a plasma can be decreased if there is a nonzero neutral-atom background density in the plasma region. This is because the ion beam that emerges from the plasma has two components. One component consists of beam ions that have not charge transferred and have traveled the entire plasma length L as ions. The other component is composed of beam ions that have charge transferred an even number of times with the neutrals and ions of the plasma, and have traveled a distance less than the total plasma length as ions. The distance they travel as neutrals is not effective in producing energy loss. Neglecting emerging beam ions resulting from four or more charge transfers, we can calculate the average path length I_1 in the plasma for beam ions, when they are ions, as follows. We assume that only double charge-transfer occurs.

We define the following variables: Q, the resonant Cs-Cs$^+$ charge-transfer cross section; n_n the neutral density; n_i the ion density; $K_n=n_nQ$; and $K_i=n_iQ$. For an ion beam of unit intensity incident on a slab of plasma of unit cross-sectional area and length L, the number of incident beam particles becoming neutrals in an element of length dx at x (cf. Fig. 12) is

$$dN_1=K_ne^{-K_nx}\,dx\ . \tag{B1}$$

The number of those dN_1 particles which becomes ions again in an element dy at y is then

$$dN_2=dN_1e^{-K_iy}K_i\,dy=K_iK_ne^{-K_nx}e^{-K_iy}\,dx\,dy\ . \tag{B2}$$

Those dN_2 particles have traveled a distance $L-(y-x)$ through the plasma as ions. The total number of incident beam particles which undergo a double charge-transfer process is

$$N_T=\int_0^L\int_{y=x}^L dN_2\ , \tag{B3}$$

while the number of particles which have traversed the entire plasma as ions is

$$N_0=e^{-K_nL}\ . \tag{B4}$$

The average distance traveled as ions by those beam ions which have undergone a double charge-transfer can be written as

$$S=\frac{1}{N_T}\int_0^L\int_{y=x}^L(L+x-y)dN_2\ . \tag{B5}$$

Finally, the average distance traversed by any beam particle as an ion is

$$L_1=(LN_0+SN_T)/(N_0+N_T)\ . \tag{B6}$$

Equation (B6) can be written as

$$L_1=\frac{Le^{-K_nL}+\int_0^L\int_{y=x}^L(L+x-y)dN_2}{e^{-K_nL}+\int_0^L\int_{y=x}^L dN_2}\ . \tag{B7}$$

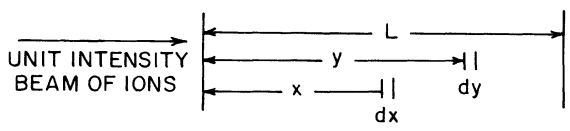

FIG. 12. Diagram used for deriving the formula giving the correction to the ion-beam path length due to a double charge-transfer process.

Evaluation of Eq. (B7) is straightforward, although time consuming. The final result is

$$L_1 = \left[\frac{K_n(K_iL-1)}{K_i(K_i+K_n)} + Le^{-K_nL} + \left(\frac{1}{K_i} - \frac{1}{K_n}\right) e^{-K_iL} + \left(\frac{K_n(1-K_iL)}{K_i(K_n+K_i)} + L + \frac{1}{K_n} - \frac{1}{K_i}\right) e^{-(K_i+K_n)L} \right]$$

$$\times \left[\frac{K_n}{K_i+K_n} + e^{-K_nL} - e^{-K_iL} + \left(\frac{K_i}{K_i+K_n}\right) e^{-(K_i+K_n)L} \right]^{-1} . \quad \text{(B8)}$$

In the limit of zero neutral density or ion density, L_1 must go to L. Equation (B8) is easily shown to have the proper limiting values, i.e.,

$$\lim_{K_i \to 0} L_1 = L \ , \quad \lim_{K_n \to 0} L_1 = L \ .$$

ACKNOWLEDGMENTS

We wish to thank Professor T. M. Miller for his assistance throughout the course of the experiment, and Lee Schumann for his help during the final stages of the work. During the early stages of this experiment, Dr. Martin Lampe was an invaluable consultant on theoretical aspects of the problem.

---

*Supported by the National Science Foundation.

†Present addresss: Esso Research Engineering Company, Linden, N.J. 07036.

‡Present address: Research Laboratories, Philip A. Hunt Chemical Corporation, Palisades Park, N.J. 07650.

[1]A number of references are cited in Sec. II, but see particularly Refs. 8–10.

[2]A preliminary report of a portion of this work appeared in I. L. Klavan, D. M. Cox, H. H. Brown, Jr., and B. Bederson, Phys. Rev. Lett. 28, 1254 (1972).

[3]M. R. Smith, and W. B. Johnson, Case Institute of Technology Report No. A-38, Cleveland, Ohio, 1965 (unpublished).

[4]J. H. Ormrod, AECL Report No. 2669, Chalk River, Ontario, 1967 (unpublished).

[5]W. Halverson, Centre d'Etudes Nucléaires Report No. EUR-CEA-FC-472, Fontenay-aux-Roses, France, 1968 (unpublished).

[6]R. J. Burke, Lawrence Livermore Laboratory, University of California at Livermore Report No. UCRL-51175, 1972 (unpublished).

[7]M. Caby-Eyaud, J. Phys. (Paris) 31, 445 (1970).

[8]I. P. Shkarofsky, T. W. Johnston, and M. P. Bachyinski, *The Particle Kinetics of Plasmas* (Addison-Wesley, Reading, Mass., 1966).

[9]D. C. Montgomery and D. A. Tidman, *Plasma Kinetic Theory* (McGraw-Hill, New York, 1964).

[10]S. T. Butler and M. J. Buckingham, Phys. Rev. 126, 1 (1962).

[11]The choice of an arbitrary cutoff at a maximum impact parameter is discussed by R. S. Cohen, L. Spitzer, and P. Routly, Phys. Rev. 80, 230 (1950). This cutoff is generally taken to be (Refs. 8 and 13) the plasma Debye shielding length, i.e., the effective range for individual Coulomb collisions.

[12]A. Chandrasekhar, Rev. Mod. Phys. 15, 1 (1943).

[13]M. N. Rosenbluth, W. M. MacDonald, and D. L. Judd, Phys. Rev. 107, 1 (1957).

[14]H. Grad, in *Proceedings of the Fifth International Conference on Ionization Phenomena in Gases*, edited by H. Maecker (North-Holland, Amsterdam, 1962), Vol. 2, p. 1630.

[15]L. Spitzer, *Physics of Fully Ionized Gases*, 2nd ed. (Wiley-Interscience, New York, 1962).

[16]T. Kihara and O. Aono, J. Phys. Soc. Jap. 18, 837 (1963).

[17]R. M. May, Phys. Rev. 135, A1009 (1964).

[18]W. B. Thompson and J. Hubbard, Rev. Mod. Phys. 32, 714 (1960).

[19]A. G. Sitenko and Yu-Mai Chien, Zh. Tekhn. Fiz. 32, 1324 (1962) [Sov. Phys.—Tech. Phys. 7, 978 (1963)].

[20]J. Hubbard, Proc. R. Soc. A 260, 114 (1961); 261, 371 (1962).

[21]A. Aono, Phys. Fluids 11, 341 (1968) and references therein.

[22]A. Aono, Phys. Soc. Jap. 17, 853 (1962); T. Kihara and O. Aono, J. Phys. Soc. Jap. 18, 837 (1963); T. Kihara, O. Aono, and Y. Itikawa, J. Phys. Soc. Jap. 18, 1043 (1963); Y. Itikawa, J. Phys. Soc. Jap. 18, 1499 (1963); T. Kihara, J. Phys. Soc. Jap. 19, 108 (1964).

[23]Y. Itikawa and O. Aono, Phys. Fluids 9, 1259 (1966).

[24]F. Perkins, Phys. Fluids 8, 1361 (1965).

[25]M. N. Saha, Proc. R. Soc. Lond. A99, 135 (1921).

[26]H. Dreicer, *Proceedings of the Conference on Controlled Thermonuclear Reactions*, TID-7503, Princeton, 1955 (unpublished).

[27]L. Enriques and F. Magistrelli, Rev. Sci. Instrum. 35, 1708 (1964).

[28]D. Balfour, D. A. Hart, and J. A. Haynes, in *Proceedings of the Seventh International Conference on Phenomena in Ionized Gases, Belgrade, 1965*, Vol. 2, p. 235 (unpublished).

[29]L. Agnew, and C. Summers, Rev. Sci. Instrum. 37, 1224 (1966).

[30]E. Gray, thesis (New York University, 1966) (unpublished).

[31]I. Langmuir and K. H. Kingdon, Proc. R. Soc. Lond. A107, 61 (1925).

[32]J. B. Taylor, Z. Phys. 57, 242 (1929).

[33]S. Datz and E. H. Taylor, J. Chem. Phys. 25, 389 (1956).

[34]O. Heinz and R. T. Reaves, Rev. Sci. Instrum. 39, 1229 (1968).
[35]E. A. Soa, Jenaer Jahrb. 1, 115 (1959).
[36]J. A. Simpson and C. E. Kuyatt, Rev. Sci. Instrum. 34, 265 (1963).
[37]S. Stephanakis and W. H. Bennett, Rev. Sci. Instrum. 39, 1714 (1968).
[38]*Methods of Experimental Physics*, edited by B. Bederson and W. L. Fite (Academic, New York, 1968), Vol. 7.
[39]W. R. Gentry, Yuan-Tseh Lee, and Bruch Mahan, J. Chem. Phys. 49, 1758 (1968).
[40]Lawrence L. Marino, A. C. H. Smith, and E. Caplinger, Phys. Rev. 128, 2243 (1962).
[41]Donald Rapp and W. E. Francis, J. Chem. Phys. 37, 2631 (1962).
[42]J. Perel and H. L. Daley, Phys. Rev. A 4, 162 (1971).
[43]P. L. Auer, J. Appl. Phys. 31, 2096 (1960).
[44]K. D. Sevier, *Low Energy Electron Spectroscopy* (Wiley, New York, 1972).
[45]R. M. May and N. F. Cramer, Phys. Fluids 13, 1766 (1970).
[46]E. W. McDaniel, *Collision Phenomena in Ionized Gases* (Wiley, New York, 1964).
[47]R. Molof, H. Schwartz, T. Miller, and B. Bederson (private communication) (to be published).
[48]E. H. Kennard, *Kinetic Theory of Gases* (McGraw-Hill, New York, 1938).